Hindawi
Geofluids
Volume 2022, Article ID 8526755, 16 pages
https://doi.org/10.1155/2022/8526755

Research Article

Research and Application of Prefilled Concrete Wall to Reduce the Size of Stopping Mining Coal Pillar

Jiao Zhang, Shuwei Sun, Zhiqiang Wang, and Jingkai Li

School of Energy and Mining Engineering, China University of Mining and Technology (Beijing), Beijing 100083, China

Correspondence should be addressed to Jiao Zhang; zj33703370@163.com

Received 24 June 2022; Revised 2 August 2022; Accepted 9 August 2022; Published 10 September 2022

Academic Editor: Mohammed Fattah

The long-term stability and width of stopping mining coal pillar have an important influence on mine safety production. In view of the "┤" type spatial structure of stop mining position of 6105 working face in Hongshuliang Coal Mine, the mechanical equilibrium, the distribution law of stress concentration factor, and the distribution characteristics of elastic zone of "filling body-remaining stopping mining " structure are studied by means of theoretical calculation, FLAC3D numerical simulation software, and field measurement. The research shows that (1) the concrete filling body can protect the remaining stopping mining coal pillar, the surrounding rock of the retracement channel, and the surrounding rock of the main roadway, and the width formula of " filling body - remaining stopping mining coal pillar " structure is deduced; (2) in the retracement channel, increasing the internal friction angle and cohesion of coal can eliminate the spalling and large deformation of surrounding rock; (3) according to the comprehensive analysis, the width of the "filling body-remaining coal pillar" structure is 25 m, in which the width of the concrete filling body with uniaxial compressive strength of 50 MPa is 6 m, and the recovery rate of stopping mining coal pillar is increased by 52.5%; and (4) field measurement shows that in the retracement channel, there is no spalling and large deformation. In the auxiliary main haulage roadway, the maximum deformations of roof, floor, solid coal side, and stopping mining coal pillar side are 46 mm, 18.4 mm, 55.9 mm, and 74.8 mm, respectively.

1. Introduction

In the process of working face mining, due to the need of technology and safety, different kinds of coal pillars are involved, such as stopping mining protection coal pillar, main haulage roadway protection coal pillar, and roadway protection coal pillar. The stability of these coal pillars plays an important role in the safe production of coal mines. At present, large-size protective coal pillars are widely used, resulting in serious waste of coal resources. Taking Tongxin Coal Mine and Tashan Coal Mine as examples, the width of stopping coal pillar is blindly set according to work experience, the width of stopping coal pillar is 200 m ~230 m, and the coal loss is about 1.6 million tons [1]. Therefore, many scholars have studied the size of protective coal pillar. Wang et al. [2], An-ye et al. [3], Jinqiang et al. [4], and other scholars have studied the law of microseismic activity in the coal pillar region and concluded that the microseismic activity of the coal pillar reduces the stability of the coal pillar. Sun et al. [5], Han et al. [6], Chen et al. [7], Zhang et al. [8], and other scholars believe that the advance support stress is the main factor affecting the size of coal pillar, and it is determined that the boundary line where the advance support stress is 1.1 times of the stress in original rock is taken as the basis for designing the size of stopping mining protection coal pillar. Yansheng [9], Liu et al. [10], Li et al. [11], Yi et al. [12], and other scholars studied the movement law of overlying strata in the mining process and analyzed the type and mechanism of mine pressure bump. It is considered that when the stress in the coal pillar is more than 1.5 times of the uniaxial compressive strength of the coal body,

the coal pillar is in danger of impact pressure. Therefore, the critical lower limit of coal pillar size is that the bearing stress of coal pillar is 1.5 times of the uniaxial compressive strength of coal mass. Shi et al. [13], Fang-Tian et al. [14], Chen et al. [15], and other scholars studied the failure characteristics of coal pillar and determined the size of coal pillar based on the width of elastic zone of coal pillar.

The above research mainly studies the stability of protecting coal pillar from four aspects: the microseismic activity of coal pillar, the advance support stress of working face, the law of overlying strata, and the width of elastic zone of coal pillar but seldom considers the weakening effect of time effect on the strength of protective coal pillar; that is, the uniaxial compressive strength of coal pillar has a decreasing trend under the action of static load for a long time. Taking the 6015 working face of Hongshuliang Coal Mine as the engineering background, this paper adopts the methods of theoretical calculation and FLAC3D simulation to preexcavate a retracement channel at the reasonable position of 6105 working face. Theoretical analysis, numerical simulation, and field measurement are used to determine the reasonable position of the preexcavation retracement channel in 6105 working face. On the basis of considering the weakening effect of time effect on stopping mining coal pillar, the "filling body-remaining stopping mining coal pillar" structure is formed by replacing partial stopping mining coal pillar with concrete filling body in the retracement channel. Applying the synergistic bearing effect of "filling body-remaining stopping mining coal pillar" structure can reduce the deformation of roadway surrounding rock, enhance the long-term stability of stopped coal pillar, and reduce the size of stopping mining coal pillar. In engineering practice, this method eliminates the problem of large deformation of retracement channel surrounding rock, increases the stability of the auxiliary main haulage roadway surrounding rock, and increases the recovery rate of stopping mining coal pillar by 52.5%.

2. Engineering Background

The average thickness of No. 6 coal seam in Hongshuliang Coal Mine is 5.4 m. The buried depth of No. 6 coal seam is between 130.2 m and 187.5 m, and the average depth is 160 m. The distance between the auxiliary main haulage roadway and the main haulage roadway is 40 m, and the cross-section specification of two roadways is 5 m × 5.4 m in the No. 6 coal seam. The strike length and dip length of 6014 and 6105 working faces are 200 m and 1100 m, respectively, the 6104 working face has been mined out, and the 6105 working face is the continuous working face. After monitoring, the average periodic pressure distance of the 6104 and 6105 working face is 20 m, and the distance between the stopping mining position of the 6104 working face and the last periodic pressure of the working face is 10 m, while the distance between the stop mining position of the 6104 working face and the auxiliary main haulage roadway is 50 m. It is planned to arrange a preexcavation retracement channel in the suitable position of 6105 working face, and the section specification of the retracement channel is 5 m × 5.4 m. The layout of the working face and the lithology of the roof and floor of the working face are shown in Figure 1.

3. Spatial Mechanical Model of Stopping Mining Position

3.1. Stability Analysis of Stopping Mining Coal Pillar. In order to determine the size of the stopping mining coal pillar, it is necessary to analyze the broken structure of the overlying strata of the working face. According to the filling degree of the equivalent direct roof to the mined-out area [16], the fracture structure of the roof of the working face can be divided into step rock beam structure and masonry beam structure. According to Minggao et al.'s research results [17], the rotating amount Δ_X of broken rock block and rotating amount $\Delta_{\max}$ of fracture structure are, respectively, as follows:

$$\Delta_x = m - (K_s - 1)h_1, \tag{1}$$

$$\Delta_{\max} = h_2 - L\sqrt{2(q_0 + \gamma_2 h_2)/[\sigma]}, \tag{2}$$

where m represents the thickness of coal seam, m; K_s represents the broken expansion coefficient of rock formation; h_1 represents the height of thick and hard strata from the coal seam, m; L represents the breaking distance of thick and hard rock stratum, m; q_0 represents the overburden load borne by the thick and hard rock beam, MPa; γ_2 represents the volumetric weight of thick and hard rock beam, kN/m^3; h_2 represents the thickness of thick and hard rock beam, kN/m^3; and $[\sigma]$ represents the compressive strength of rock blocks after breaking of thick and hard strata, MPa.

The formation condition of step rock beam structure of thick and hard rock stratum is $\Delta_X \geq \Delta_{\max}$; otherwise, the masonry beam structure is formed.

According to the field practice of 6105 working face, substituting the mechanical parameters in Table 1 into formulas (1) and (2), it is calculated that $\triangle x = 3.68$ m, $\triangle \max = 7.5$ m ~ 8.2 m, and $\Delta_x < \Delta_{\max}$ are satisfied. Therefore, the basic roof fracture structure of 6105 working face is the masonry beam structure.

Without considering the occurrence characteristics of coal body and geological structure, coal seams and rock strata are regarded as isotropic continuous, uniform, isotropic, and completely elastic materials. In the stopping mining position of the working face, the structure and stress state between the roof strata and the stopping mining coal pillar are analyzed, and the mechanical schematic diagram of the stopping mining coal pillar without instability is shown in Figure 2.

As shown in Figure 2, D represents the width of the stopping mining coal pillar, a represents the width of the protected roadway, h_3 represents the distance between the basic roof of the working face and the surface, H represents the buried depth of the coal seam, α and β are the comprehensive movement angle of the overlying strata and the gangue contact angle of the broken strata of the goaf, respectively, and l is the cantilever beam length of the basic roof.

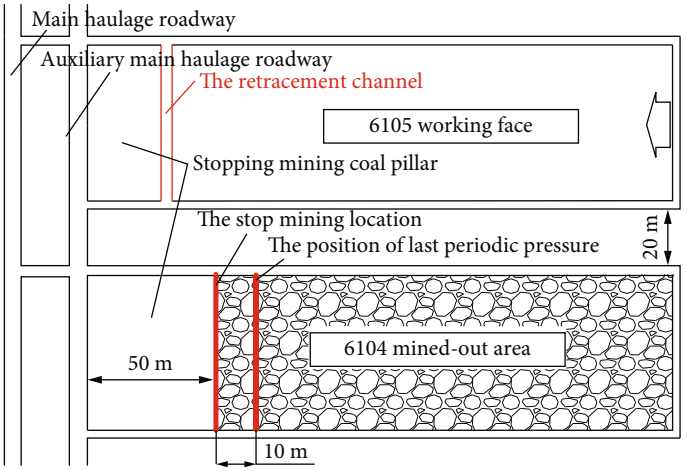

(a) Schematic diagram of working face layout

Lithology		Thickness
Siltstone		4.7 m
Kaolin		3.2 m
Sandy mudstone		2.4 m
Medium grained sandstone		12.8 m
Sandy mudstone		1.9 m
Kaolin		1.8 m
Sandstone		2.3 m
Sandy mudstone		2.6 m
Coal		5.4 m
Grit stone		5.7 m
Fine sandstone		16 m

(b) The lithology of roof and floor of working face

Figure 1: Working face layout diagram and lithology.

Table 1: Mechanical parameters of 6105 working face.

Symbol of the parameter	K_s	h_1/m	h_2/m	L/m	γ_2/kN·m^{-3}	q_0/MPa	$[\sigma_{max}]$/MPa	m/m
The value of the parameter	1.2	8.6	12.8	20	25	0.215	50.3	5.4

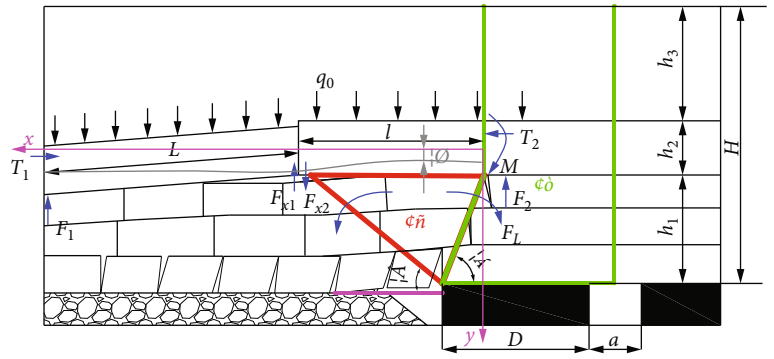

Figure 2: Spatial structure and mechanical model of stopping mining coal pillar.

The stopping mining position, stopping mining coal pillar, and suspended structure of basic roof constitute the spatial structure of "┤" type. In the "┤" type spatial structure, the stopping mining coal pillar is used as the supporting body in the vertical direction, and the cantilever rock beam and the hinged structure of the broken rock block are the main transmission bodies to transfer the overlying strata gravity in the horizontal direction. The hinged structure of the broken rock block and the cantilever rock beam are squeezed by rock masses on both sides to form horizontal thrust T_1 and T_2. In the vertical direction, the supporting force of the contact gangue point and the fixed end is simplified as the concentrated force F_1 and F_2, and the deflection between the cantilever beam structure and the broken rock block structure is recorded as ω. Assuming that the slow deformation of "┤" type structure can be approximated to the equilibrium structure, the mechanical equilibrium condition is established.

$$\begin{cases} \sum F(x) = 0, \\ \sum F(y) = 0, \\ \sum M(F) = 0. \end{cases} \tag{3}$$

The extrusion between the adjacent rock beams forms a pair of horizontal thrust, which meets the following equilibrium conditions:

$$T_1 = T_2. \tag{4}$$

Ignoring the influence of the rotation of the broken rock block, the concentrated force F_1 of contact gangue point, the concentrated force F_2 of fixed end, cantilever rock beam structure, and the hinged structure of the broken rock block maintain mechanical balance:

$$F_1 + F_2 = (q_0 + \gamma_2 h_2)(l + L). \tag{5}$$

Due to the extrusion of adjacent rock beams, the friction forces F_{X1} and F_{X2} are formed in the vertical direction. Broken rock blocks maintain equilibrium of force in the vertical direction:

$$\begin{cases} F_1 + F_{x1} = (q_0 + \gamma_2 h_2)L, \\ F_{x1} = F_{x2}. \end{cases} \tag{6}$$

The expression of the concentrated force F_2 at the fixed end can be obtained from the formulas (3)–(6):

$$F_2 = \frac{1}{2}(q_0 + \gamma_2 h_2)(l + L). \tag{7}$$

From the formula (7), it can be known that F_2 is a function of $l \in [0, L]$, and F_2 belongs to the transfer load or additional load formed by the mining process.

According to the area II in Figure 2, the gravity of the rock stratum that is not affected by obvious mining influence is estimated.

$$G = \frac{\bar{\gamma} h_1}{2}(2D + a - h_1 \cot \alpha) + \bar{\gamma}(h_3 + h_2)\left(D + \frac{a}{2} - h_1 \cot \alpha\right), \tag{8}$$

where G represents the gravity of the rock stratum, kN; and $\bar{\gamma}$ represents the average volumetric weight, kN/m^3.

Area I in Figure 2 is a collapsed rock layer under the thick and hard rock. Due to the existence of the hard rock layer, this part of the collapsed rock layer can still form a hinged structure at the boundary of the stope, and the weight of area I is transferred to the stopping mining coal pillar and the falling bottom gangue, respectively. F_L is approximately 1/2 of the weight of area I.

$$F_L = \frac{\bar{\gamma} h_1}{4}(h_1 \cot \alpha + h_1 \cot \beta). \tag{9}$$

The total gravity of the overlying strata carried by the stopping mining coal pillar is approximately expressed as

$$W = G + F_2 + F_L, \tag{10}$$

where W represents total gravity of the overlying strata carried by the stopping mining coal pillar.

Under static condition, the average stress P of stopping mining coal pillar is

$$P = \frac{W}{D} = \bar{\gamma} H + \frac{\bar{\gamma} H}{D}\left(\frac{a}{2} - h_1 \cot \alpha\right) + \frac{(q_0 + \gamma_2 h_2)(l + L)}{2D} + \frac{\bar{\gamma} h_1^2 (\cot \beta + 3 \cot \alpha)}{4D}. \tag{11}$$

Mining practice and theoretical research [18] show that the movement of basic roof can produce dynamic load effect in the process of working face mining. The suspended rock beam of basic roof produces flexure deformation and accumulates energy, and the relationship between the accumulated energy U and deflection ω is as follows:

$$U = \int_0^l \omega(q_0 + \gamma_2 h_2)dx = \int_0^l \left[\frac{(q_0 + \gamma_2 h_2)^2 x^2}{24EI} \cdot \left[\left(6l^2 + x^2 - 4lx\right) - 2l(3l - x)\right]\right]dx, \tag{12}$$

where E represents the elastic modulus, GPa, and I represents the inertial moment.

Sort out the formula (12) and get

$$U = \frac{19(q_0 + \gamma_2 h_2)^2 l^5}{12E{h_2}^3}. \tag{13}$$

It can be seen from the expression of formula (13) that the accumulated elastic energy of the basic roof has a 5th power relationship with the length of its cantilever beam, and the released elastic energy is partially transferred to the supporting coal body to form dynamic load, which is related to the static load of the coal body. The "dynamic-static" load superposition is generated, which reduces the stability of the coal pillar.

In general, the dynamic-load stress P_D is about k_D times the static-load stress P, that is, $P_D = K_D P$. Therefore, considering the dynamic-static loading stress condition, the average stress P_z of stopping mining coal pillar is approximately as follows:

$$P_Z = P + P_D = (1 + K_D)\left[\bar{\gamma} H + \frac{\bar{\gamma} H}{D}\left(\frac{a}{2} - h_1 \cot \alpha\right) + \frac{(q_0 + \gamma_2 h_2)(l + L)}{2D} + \frac{\bar{\gamma} h_1^2 (\cot \beta + 3 \cot \alpha)}{4D}\right]. \tag{14}$$

The strength of the stopping mining coal pillar is calculated according to the Bieniawski formula:

$$\sigma_q = \sigma_j\left(0.64 + 0.54\frac{D}{m}\right), \tag{15}$$

where σ_j represents the uniaxial compressive strength of coal, MPa.

Table 2: Mechanical parameters of stopping mining coal pillar.

Symbol of the parameter	k_x	H/m	a/m	K_D	l/m	α/°	β/°	σ_j/MPa	γ/kN·m^{-3}	γ/kN·m^{-3}	D/m
The value of the parameter	0.75	160	5	2.9	15	83	60	8	25	25	10~30

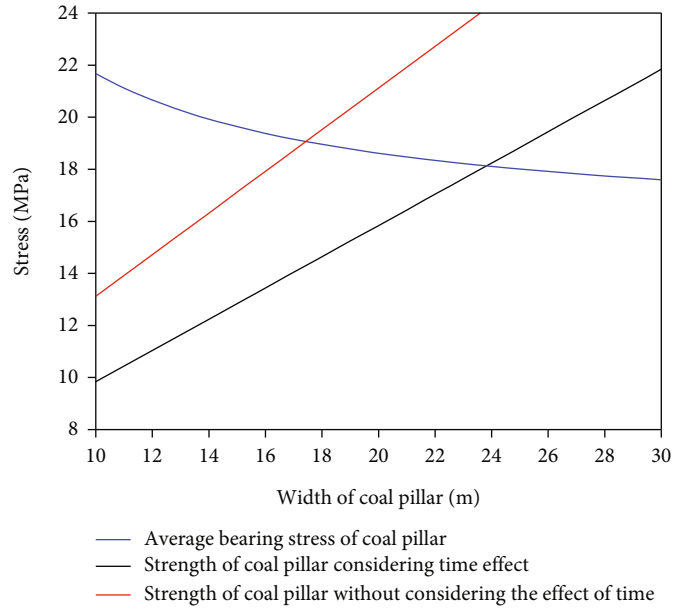

Figure 3: The relationship between the width, strength, and the average stress of the stopping mining coal pillar.

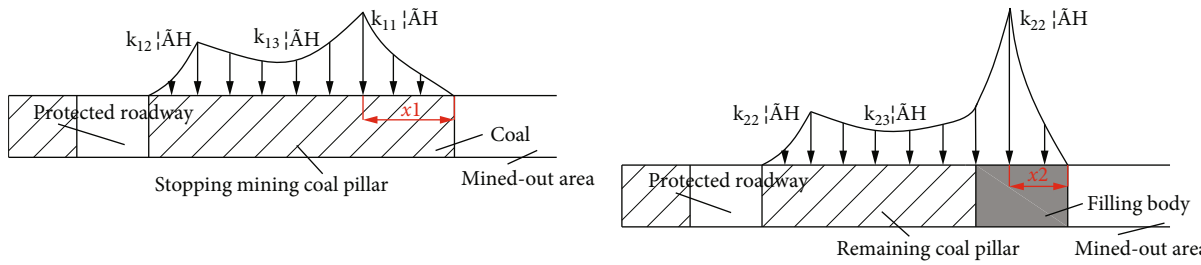

(a) Stress distribution of coal pillar

(b) Stress distribution of filling body-remaining coal pillar

Figure 4: Mechanical model of stopping mining coal pillar.

Simultaneous equations (14) and (15) can solve the width of stopping mining coal pillar to maintain stability.

$$(1+K_D)\left[\bar{\gamma}H+\frac{\bar{\gamma}H}{D}\left(\frac{a}{2}-h_1\cot\alpha\right)+\frac{(q_0+\gamma_2h_2)(l+L)}{2D}+\frac{\bar{\gamma}h_1^2(\cot\beta+3\cot\alpha)}{4D}\right]=\sigma_j\left(0.64+0.54\frac{D}{m}\right). \tag{16}$$

In order to maintain the long-term stability of the coal pillar, the time effect should be taken into account. Under the long-term static load, the uniaxial compressive strength of the coal pillar decreases obviously [19–22]. Considering the reduction degree of uniaxial compressive strength of coal, the width of stopping mining coal pillar to maintain long-term stability is as follows:

$$(1+K_D)\left[\bar{\gamma}H+\frac{\bar{\gamma}H}{D}\left(\frac{a}{2}-h_1\cot\alpha\right)+\frac{(q_0+\gamma_2h_2)(l+L)}{2D}+\frac{\bar{\gamma}h_1^2(\cot\beta+3\cot\alpha)}{4D}\right]=k_x\sigma_j\left(0.64+0.54\frac{D}{m}\right), \tag{17}$$

where k_x represents the reduction coefficient of uniaxial compressive strength of coal.

By substituting the mechanical parameters of the stopping mining coal pillar in Tables 1 and 2 into the formulas (16) and (17), the relationship between the width, strength, and average stress of the stopping mining coal pillar can be obtained, as shown in Figure 3.

Table 3: Mechanical parameters of the "filling body-remaining coal pillar" structure.

Lithology	Compressive strength (σ_h)/MPa	Density (ρ)/ kN·m^{-3}	Elastic modulus (E)/GPa	Poisson's ratio (μ)	Cohesion (C)/MPa	Internal friction angle (φ)/°	Width (s_1)/m	Width (s_2)/m
Filling body	50	2456	11	0.22	3.33	44	10~22	
Filling body	40	2456	9.3	0.22	2.95	40	10~22	
Filling body	30	2456	5.9	0.23	2.65	37	10~22	
Coal pillar	8	1440	0.982	0.23	1.7	28		15~ 3

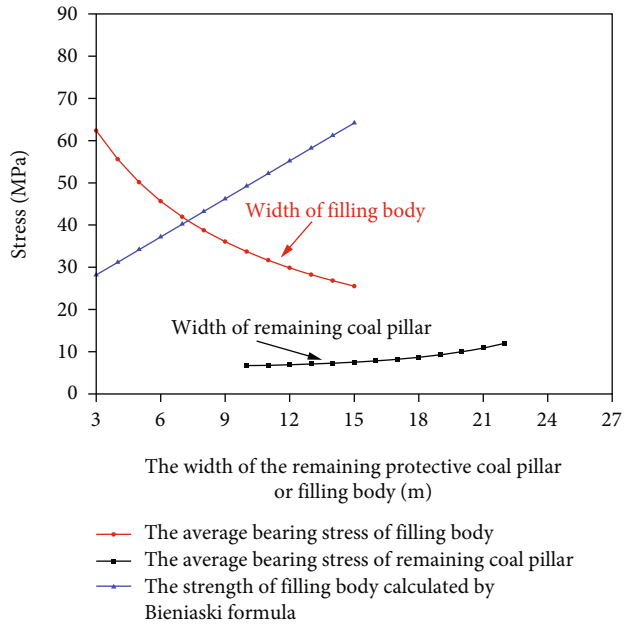

(a) Filling body with compressive strength of 50 MPa

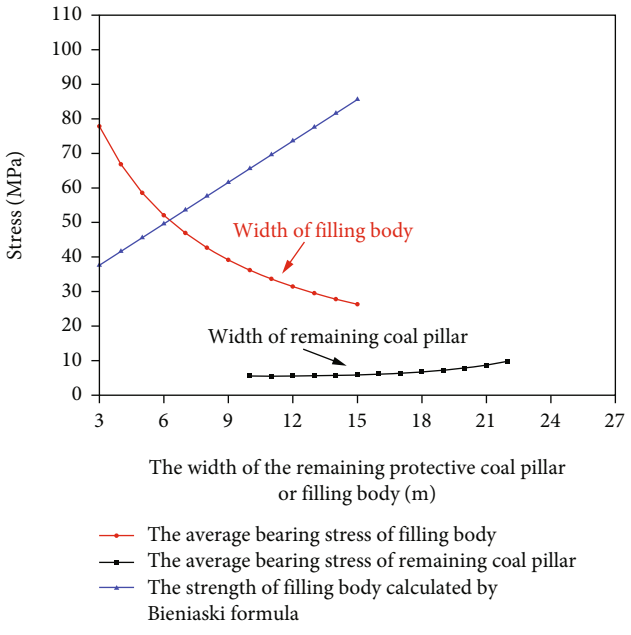

(b) Filling body with compressive strength of 40 MPa

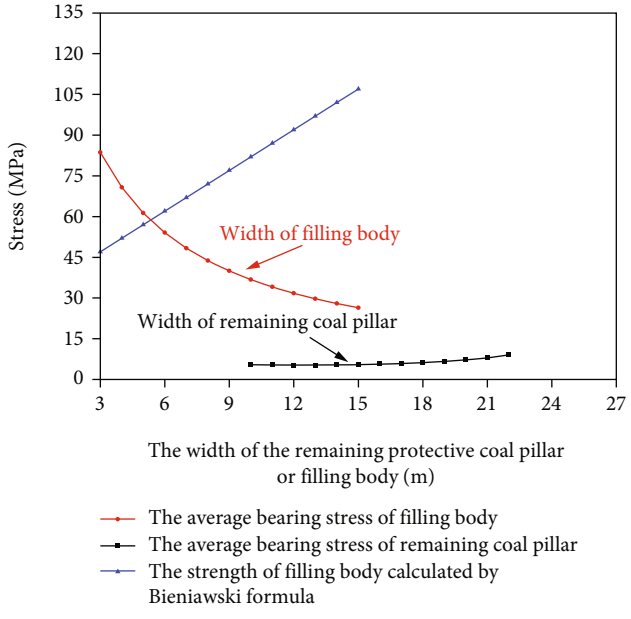

(c) Filling body with compressive strength of 50 MPa

Figure 5: Average stress shared by filling body and remaining coal pillar.

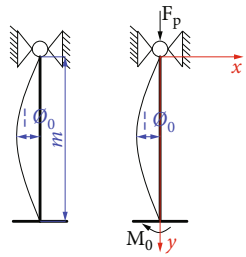

Figure 6: Mechanical model of the solid coal side of the retraction channel.

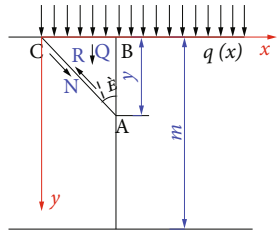

Figure 7: Mechanical model of the solid coal side of the retracement roadway.

As shown in Figure 3, with the increase of the width of stopping mining coal pillar, the strength of stopping mining coal pillar increases, while stopping mining coal pillar bearing average stress decreases. Without considering the time effect to reduce the coal strength, when the width of the coal pillar is 17 m ~18 m, the strength curve of the coal pillar intersects the curve of the average bearing stress of the coal pillar, and the average bearing stress of the coal pillar is 19 MPa. With considering the time effect to reduce the coal strength, when the width of the coal pillar is 24 m ~25 m, the strength curve of the coal pillar intersects the curve of the average bearing stress of the coal pillar, and the average bearing stress of the coal pillar is 18 MPa. Because the service time of stopping mining coal pillar is generally one year or more, so the width of stopping mining coal pillar is at least 25 m in consideration of safety.

3.2. Synergistic Effect of Filling Body and Remaining Coal Pillar. In the stopping mining coal pillar, the mined-out area side of stopping mining coal pillar bears higher stress, as shown in Figure 4(a) . The study shows [23–26] that the filling body replaces part of the stopping mining coal pillar, the filling body and the remaining stopping mining coal pillar share the overlying rock mass load, and more high stress is transferred to the filling body, while the stress shared by the remaining coal pillar tends to decrease, as shown in Figure 4(b). In Figure 4, $k_{11} < k_{12}, k_{12} < k_{22}, k_{13} > k_{23}, x_1 > x_2$, indicating that the stability of stopping mining coal pillar can be improved by "filling body-remaining pillar" structure sharing the load.

The filling body replaces part of the stopping mining coal pillar, and the filling body and the remaining coal pillar share the load of the overlying rock mass. The following formula can be obtained from the static equilibrium condition and formula (14)

$$\begin{cases} DP_Z = s_1\overline{P_1} + s_2\overline{P_2}, \\ D = s_1 + s_2, \end{cases} \tag{18}$$

where s_1 represents width of the remaining stopping mining coal pillar, m; s_2 represents width of filling body, m; $^{-}P_1$ represents remaining stopping mining coal pillar sharing average stress, MPa; and $^{-}P_2$ represents filling body sharing average stress, MPa.

Through the calculation [27], it can be obtained that the stress shared by the filling body and the remaining stopping mining coal pillar are, respectively, as follows:

$$\begin{cases} \overline{P_1} = \dfrac{DP_Z}{s_1 + s_2 b_0}, \\ \overline{P_2} = \dfrac{DP_Z b_0}{s_1 + s_2 b_0}. \end{cases} \tag{19}$$

In the formula (19), the b_0 is represented by the following expression:

$$\begin{cases} b_0 = \dfrac{E_2\left(1-\mu_1^2-b_1\mu_1-c_1\mu_1^2\right)+E_1 b_1\mu_2(1+\mu_2)}{E_1\left(1-\mu_2^2-b_2\mu_2-b_2\mu_2^2\right)+E_2 b_2\mu_1(1+\mu_1)}, \\ b_1 = \dfrac{E_2 s_1\mu_1(1+\mu_1)}{E_2 s_1\left(1-\mu_1^2\right)+E_1 s_2\left(1-\mu_2^2\right)}, \\ b_2 = \dfrac{s_2\mu_2(1+\mu_2)}{s_1\mu_1(1+\mu_1)} b_1, \end{cases} \tag{20}$$

where E_1 represents the elastic modulus of coal, GPa; E_2 represents the elastic modulus of the filling body, GPa; μ_1 represents the Poisson ratio of coal; and μ_2 represents Poisson ratio of filling body.

The strength of the filling body is calculated according to the Bieniawski formula:

$$\sigma_H = \sigma_h\left(0.64 + 0.54\frac{s_2}{m}\right), \tag{21}$$

where σ_h represents the uniaxial compressive strength of the filling body, MPa.

Simultaneous formulas (19) and (21) can obtain the relationship between the strength of the filling body and its sharing average stress:

$$\frac{DP_Z}{s_1 + s_2 b_0} \le \sigma_h\left(0.64 + 0.54\frac{s_2}{m}\right). \tag{22}$$

It can be known from the above formula that the structure of "filling body-remaining coal pillar" is related to factors such as elastic modulus, Poisson's ratio, width of remaining coal pillar, width of filling body, and uniaxial compressive strength of the concrete filling body. Therefore,

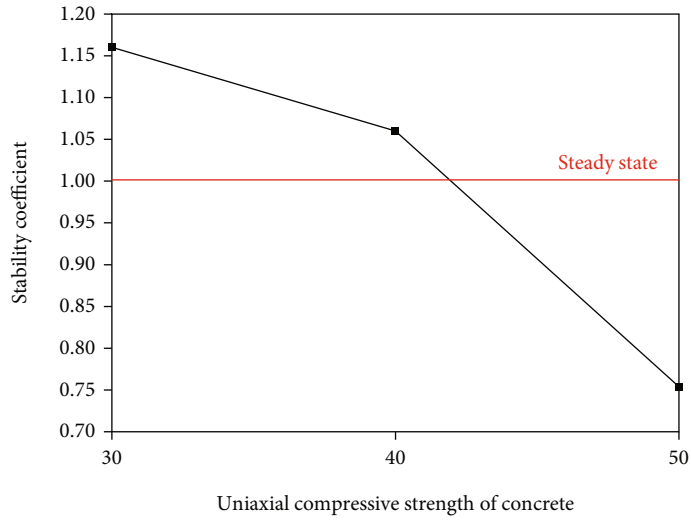

Figure 8: Balance state of coal wall.

the mechanical parameters of the filling body with different uniaxial compressive strength and mechanical parameters of remaining coal pillar in Table 3 are substituted into formulas (18)–(22), and it can be obtained that the "filling body-remaining coal pillar" structure bears average stress when filling body with different strengths replaces partially stopping mining coal pillar as shown in Figure 5.

The uniaxial compressive strengths of the filling body in Figures 5(a)–5(c) are 50 MPa, 40 MPa, and30 MPa, respectively. As the uniaxial compressive strength of the filling body decreases from 50 MPa to 30 MPa, and when the width of the filling body replacing stopping mining coal pillar increases from 3 m to 15 m, the average stress shared by the filling body decreases from 83.67 MPa to 26.4 MPa, 77.84 MPa to 26.3 MPa, and 2.343 MPa to 25.5 MPa, respectively. As the uniaxial compressive strength of the filling body decreases from 50 MPa to 30 MPa, and when the width of the remaining coal pillar decreases from 22 m to 10 m, the average stress shared by the remaining coal pillar decreases from 9.05 MPa to 5.4 MPa, 9.84 MPa to 5.54 MPa, and 9.84 MPa to 5.54 MPa, respectively.

To sum up, when the uniaxial compressive strength of the filling body decreases from 50 MPa to 30 MPa, the curve of the average stress shared by the filling body intersects the curve of the strength of the filling body when the width of the filling body is about 6 m, 7 m, and 8 m, respectively.

3.3. Failure Mechanism of Retracement Roadway. When the working face and the retracement roadway are connected, the movement state of the basic roof will have an impact on deformation of the retracement roadway. In view of the deformation and failure of the stopping mining coal pillar side in the retracement roadway, the "pressure bar" theory is used to analyze [28–30]. According to the degree of disturbance on the stopping mining coal pillar side of the retracement roadway, the mechanical model of the stopping mining coal pillar side of the retracement roadway can be divided into the form of compression bar with simple support at the top and fixed support at the bottom, as shown in Figure 6.

Table 4: The scheme of replacing partial stopping mining coal pillar with concrete filling body.

Schemes	Width of filling body/m	Width of remaining coal pillar/m	Width of stopping mining coal pillar/m
1	0	25	25
2	4	21	25
3	5	20	25
4	6	19	25
5	7	18	25

Taking the centroid of the y-axis section as the center, the moment balance equation is established.

$$M_x = F_p\omega_0 - \frac{M_0 y}{m}, \tag{23}$$

where M_x represents bending moment at the centroid of the x-axis section, kN·m; F_p represents the vertical stress of the stopping mining coal pillar side, MPa; M_0 represents the moment of force at fixed end, N·m; and ω_0 represents disturbance degree of coal wall, mm.

From the following differential equations,

$$\mathrm{EI}\omega_0'' = -M_x. \tag{24}$$

The formula (24) is substituted into the formula (23) to obtain

$$\omega_0'' + \frac{F_p}{\mathrm{EI}}\omega_0 = \frac{M_0 y}{m\mathrm{EI}}. \tag{25}$$

The general solution of formula (25) is

$$\omega_0 = A\cos\sqrt{\frac{F_p}{\mathrm{EI}}}y + B\sin\sqrt{\frac{F_p}{\mathrm{EI}}}y + \frac{M_0 y}{F_p h}. \tag{26}$$

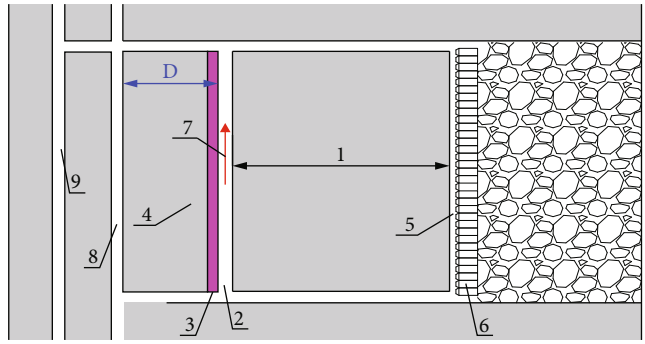

1: safety distance; 2: retracement channel; 3: filling body; 4: remaining coal pillar; 5: mining working face; 6: hydraulic support; 7: axial direction of retracement channel; 8: the auxiliary main haulage roadway; 9: the main haulage roadway; D: the sum of the width of the coal pillar and the wall.

Figure 9: Layout diagram of retracement channel and filling body.

According to the boundary conditions,

$$\begin{cases} y = 0, & \omega_0 = 0, \\ y = m, & \dfrac{d\omega}{dx} = 0. \end{cases} \tag{27}$$

Substituting the boundary conditions into formula (26), we get

$$\omega_0 = \frac{M_0}{F_p}\left[\frac{y}{m} + 1.02 \sin\left(4.49\frac{y}{m}\right)\right]. \tag{28}$$

In formula (28), when $\sin(4.49(y/m)) = 1$, the disturbance degree reaches the maximum value, that is, $y = 0.35$ m, and destruction occurs in the middle and upper part of the stopping mining coal pillar side of the retracement roadway.

The failure form of the stopping mining coal pillar side of the retracement roadway can be simplified to a plane block structure, the coal body occurs shear sliding under the action of dead weight and roof pressure, and its mechanical model is shown in Figure 7.

The weight of block ABC is

$$\begin{cases} Q = \dfrac{\rho y^2}{2} \tan\theta, \\ \tan\theta = \dfrac{x}{y}, \end{cases} \tag{29}$$

where ρ represents the density of coal, kg/m^{-3}, and φ represents internal friction angle of coal, °; $\theta = 45° - \varphi/2$.

The pressure of the overlying strata on the triangular block is [31]

$$q(x) = (K-1)\gamma H e^{-2f/m\eta(d_x - x)} + \gamma H, \tag{30}$$

where d_x represents the distance between the location of the last fracture of the basic roof and point C, m; K represents the coefficient of stress concentration; f represents the friction coefficient, $f = \tan(\varphi)$; λ represents the confining pressure coefficient; and $\eta = 1/\lambda$.

According to the mechanical equilibrium condition, the sliding force N and antiskid force R are, respectively, as follows:

$$N = \frac{\rho y^2}{2} \sin\theta + \left[(K-1)\gamma H e^{-2f/m\eta(d_x - x)} + \gamma H\right] y \sin\theta, \tag{31}$$

$$R = \left(\frac{\rho y^2}{2} + \left((K-1)\gamma H e^{-2f/m\eta(d_x - x)} + \gamma H\right) y\right) \cdot \tan\theta \sin\theta \tan\varphi + C\frac{y}{\cos\theta}, \tag{32}$$

where C represents the cohesive force of coal.

The equilibrium state of the coal wall can be obtained by substituting the formulas (31) and (32) into the following formulas:

$$E = \frac{N}{R} = \frac{\left(\rho y^2 + 2y\left((K-1)\gamma H e^{-2f/m\eta(d_x - x)} + \gamma H\right)\right)\tan\theta}{\left(\rho y^2 + 2y\left((K-1)\gamma H e^{-2f/m\eta(d_x - x)} + \gamma H\right)\right)\tan^2\theta \tan\varphi + 2Cy}. \tag{33}$$

The formula (33) shows that the limit equilibrium state of the coal wall is related to the internal friction angle and cohesion of the coal body.

Substituting mechanical parameters of Table 3, $H = 160$ m, $K = 4$, and $\lambda = 0.33$, into formula (33) is as follows. The relationship among equilibrium state of coal wall, internal friction angle, and cohesion can be obtained, as shown in Figure 8.

As shown in Figure 8, with the increase of internal friction angle and cohesion, the stopping mining coal pillar side of the retracement channel gradually changes from the rib spalling state to the limit equilibrium state. When the uniaxial compressive strength of the concrete filling body is 30 MPa, 40 MPa, and 50 MPa, the limit equilibrium coefficient of the stopping mining coal pillar side in the retracement roadway is 1.16, 1.06, and 0.754, respectively.

Table 5: Mechanical parameters of rock strata.

Lithology	Density kg/m^{-3}	Bulk modulus/GPa	Shear modulus/GPa	Cohesion/MPa	Internal friction angle/°	Tensile strength/MPa
Siltstone	2500	5.56	3.82	1.5	34	2.02
Kaolin	2500	1.82	1.04	0.42	33	1.2
Sandy mudstone	2400	4.85	2.91	1.58	33	1.75
Sandstone	2500	7.42	5.33	2	34	4.07
Sandy mudstone	2400	4.85	2.91	1.58	33	1.75
Kaolin	2500	1.82	1.04	0.42	33	1.2
Sandstone	2500	5.56	3.82	1.5	34	2.02
Sandy mudstone	2400	4.85	2.91	1.58	33	1.75
Coal	1440	0.8	0.5	1.7	28	0.4
Grit stone	2300	5.32	3.78	2.5	31	3.1
Fine sandstone	2520	3.14	1.71	1.91	35	2.9
Filling body	2456	6.58	4.51	3.33	44	2.1

Therefore, the concrete filling body with uniaxial compressive strength of 50 MPa can eliminate the problems of spalling and large deformation of the retracement roadway.

4. Numerical Simulation Analysis of Stopping Mining Coal Pillar

4.1. Scheme of Numerical Simulation. From the above, in order to ensure the long-term stability of the stopping mining coal pillar, the width of the stopping mining coal pillar is at least 25 m. In the "filling body-remaining coal pillar" structure, when the uniaxial compressive strength of the concrete filling body is 30 MPa, 40 MPa, and 50 MPa, the reasonable width of the filling body is 8 m, 7 m, and 6 m, respectively, and the mechanical equilibrium coefficients of the stopping mining coal pillar side in the retracement roadway are 1.16, 1.06, and 0.754, respectively. Therefore, based on a comprehensive analysis of the limit equilibrium state of the retracement roadway surrounding rock and the technology of partially stopping mining coal pillar by filling body replacement, the preexcavated retracement roadway is arranged at a horizontal distance of 25 m from the auxiliary main haulage roadway, and the concrete filling body replacement partial stopping mining coal pillar is applied. The simulated scheme is shown in Table 4.

The steps of partially stopping mining coal pillar being replaced by filling body are as follows: (1) at the position of 25 m from the auxiliary main haulage roadway, the retracement channel is excavated, and the safe distance between the retracement channel and the working face is large enough. (2) After the retracement channel is completed, the coal wall on the side of the topping mining coal pillar is mined again. (3) In the axial direction of the retracement channel, the work of mining the coal wall and work of concrete filling partial stopping mining coal pillar are carried out at the same time, and the distance between the working face of mining coal wall of retracement channel and the working face of concrete filling is 10 m. The length of the concrete filled at one time is 10 m. The layout of the retracement channel and the filling body is shown in Figure 9.

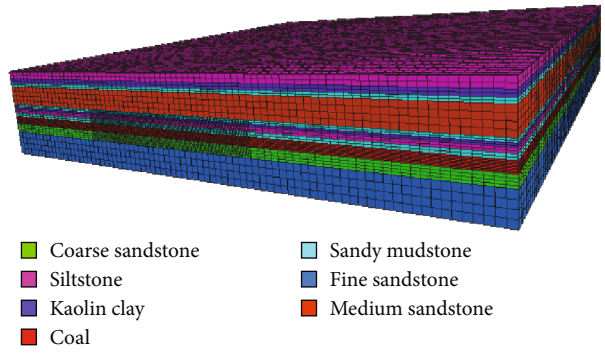

Figure 10: Three-dimensional model of numerical simulation.

4.2. Establishment of Numerical Model. According to the actual geological conditions of 6105 working face, the FLACD3D numerical model is established, and the model is the strain-softened model. The size of the model is length × width × height = 400 m × 400 m × 60 m, and the grid of the local position of the coal seam is 1 m × 0.6 m. The horizontal displacement of the x-axis and y-axis of the model is fixed, the vertical displacement of the bottom is fixed, and the top is a free surface. According to the buried depth of the coal seam, the load of 3.1 MPa is applied above the free surface to simulate the load of the overlying strata, and the mechanical parameters and model of rock strata are shown in Table 5 and Figure 10.

4.3. Mechanical Analysis of "Filling Body-Remaining Coal Pillar" Structure. When the working face is connected with the retracement channel, 50000 step static load calculation is carried out to simulate the long-term bearing capacity of stopping mining coal pillar. The stress concentration

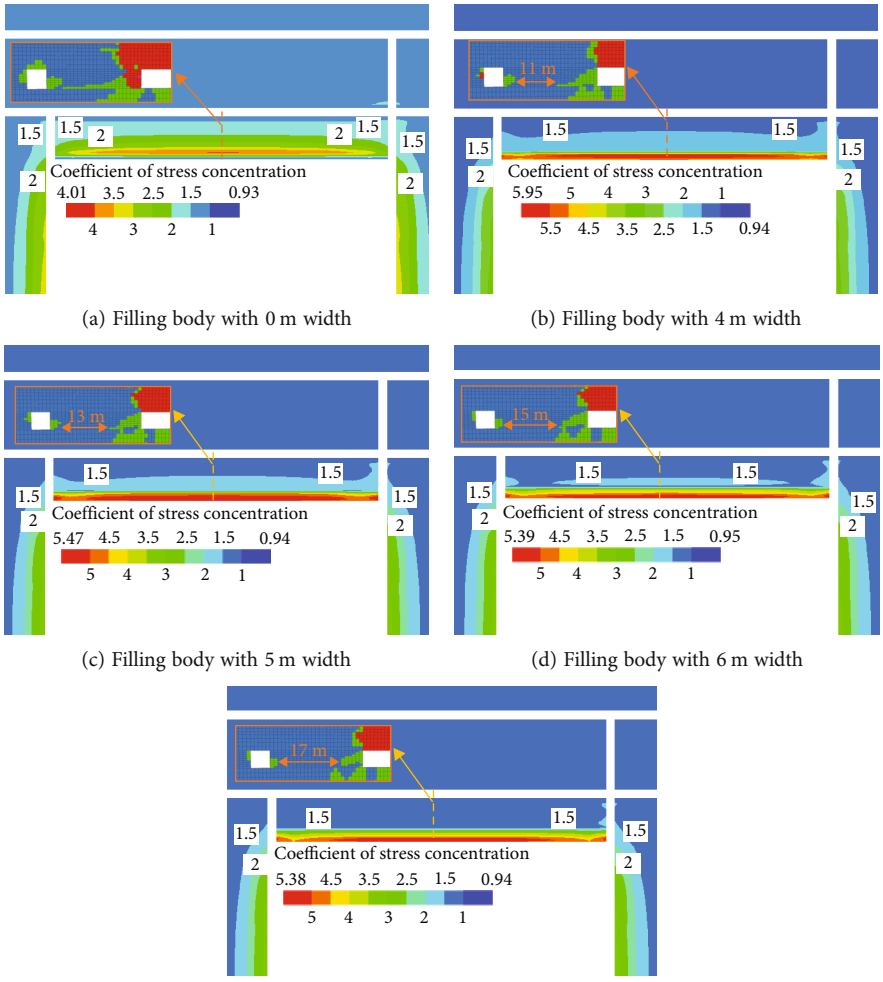

(a) Filling body with 0 m width

(b) Filling body with 4 m width

(c) Filling body with 5 m width

(d) Filling body with 6 m width

(e) Filling body with 7 m width

Figure 11: Distribution law of elastic zone and stress concentration factor.

coefficient and the distribution law of elastic zone in the "filling body-remaining coal pillar" structure are shown in Figures 11 and 12.

As can be seen from Figures 11 and 12 that with the increase of filling body width, the stress tends to decrease in the "filling body-remaining coal pillar" structure. The isoline with the stress concentration coefficient of 1.5 is used as the boundary between high stress and low stress. In the "filling body-remaining coal pillar" structure, when the width of the filling body increases from 0 m to 7 m, with the increase of the width of the filling body, the isoline with the stress concentration coefficient of 1.5 moves to the side of the stop mining position, the distance between the isoline with the stress concentration coefficient of 1.5 and the stopping position decreases from 22.2 m to 7.8 m, and the width of the elastic zone in the stopping mining pillar increases from 0 m to 17 m; that is, the ratio between the width of the elastic zone and the width of the stopping mining pillar increases from 0% to 68%.

To sum up, with the increase of the width of the filling body, the synergistic effect of the "filling body-remaining coal pillar" structure can enhance the long-term stability of the stopping mining coal pillar and reduce the influence of

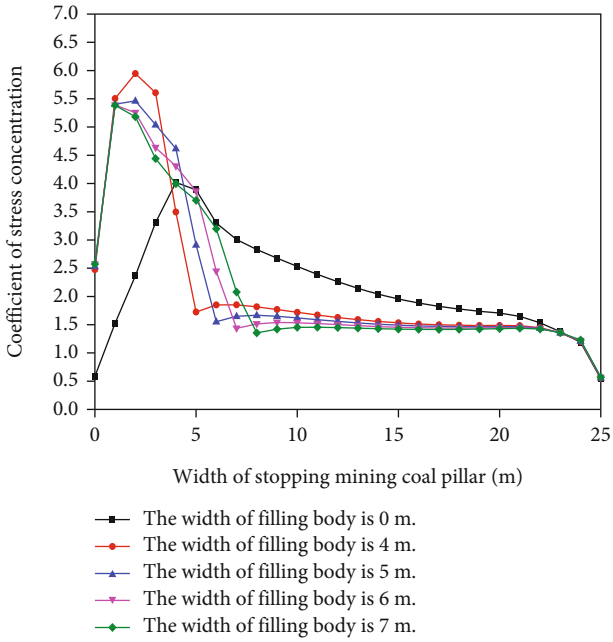

Figure 12: Curve of stress concentration coefficient.

high stress on the surrounding rock of the auxiliary main haulage roadway.

4.4. Surrounding Rock Deformation of Roadway

4.4.1. Deformation Law of Surrounding Rock in the Auxiliary Main Haulage Roadway. After the mining face is connected with the retracement channel, the static load calculation of 50000 steps is carried out to simulate the long-term stability of surrounding rock of the auxiliary main haulage roadway. When the width of the filling body in the "filling body-remaining coal pillar" structure is 0 m ~ 7 m, the deformation of the coal wall at the side of the stopping mining coal pillar in the auxiliary main haulage roadway is shown in Figure 13.

As shown in Figure 13, after long-term static load calculation, with the increase of the width of the filling body in the "filling body-remaining coal pillar" structure, the deformation of the coal wall at the side of the stopping mining coal pillar in the auxiliary main haulage roadway tends to decrease. The maximum deformation of coal wall is reduced from 39.23 mm to 29.31 mm. To sum up, the "filling body-remaining coal pillar" structure can enhance the stability of surrounding rock in the auxiliary main haulage roadway.

4.4.2. Deformation Law of Surrounding Rock of Retracement Channel. When the working face is connected with the retracement channel, the coal wall deformation at the side of the stopping mining coal pillar in the retracement channel is shown in Figure 14.

As shown in Figure 14, in the "filling body-remaining coal pillar" structure, when the width of the filling body is 0 m, the maximum compression deformation of the top and bottom of the coal wall is 77.5 mm and 22.8 mm, respectively, under the action of the roof and floor of the working face, and the maximum bulge quantity of the middle part of the coal wall is 33.5 mm. The overall deformation trend of the coal wall conforms to the "compression bar" theory. When the width of the filling body is 4 m ~ 7 m, the overall deformation trend of the filling body is compression deformation, and the compression amount at the edge of the filling body is basically the same. From the top to the bottom of the filling body, the compression of the edge of the filling body is reduced from 37.4 mm to 21.7 mm. To sum up, the problem of coal wall spalling and bulging can be eliminated by replacing partially stopping mining coal pillar with the filling body in the retracement channel.

4.5. Determination of Stopping Mining Coal Pillar Width. To sum up, in the "filling body-remaining coal pillar" structure, the high stress is concentrated on the side of the filling body, while the remaining coal pillar is in a low stress environment, and the synergistic effect between the filling body and the remaining coal pillar enhances the stability of the stopping mining coal pillar. The study shows [32, 33] that the width proportion of the elastic zone in the coal pillar is 60%, which can maintain the long-term stability of the coal pillar and the phenomenon of gas-free penetration. Therefore, according to the comprehensive analysis, the width of the "filling body-remaining coal pillar" structure is 25 m, in which the width of the concrete is 6 m, which can ensure the long-term stability of the stopping mining coal pillar, and simulation result is consistent with the theoretical calculation result.

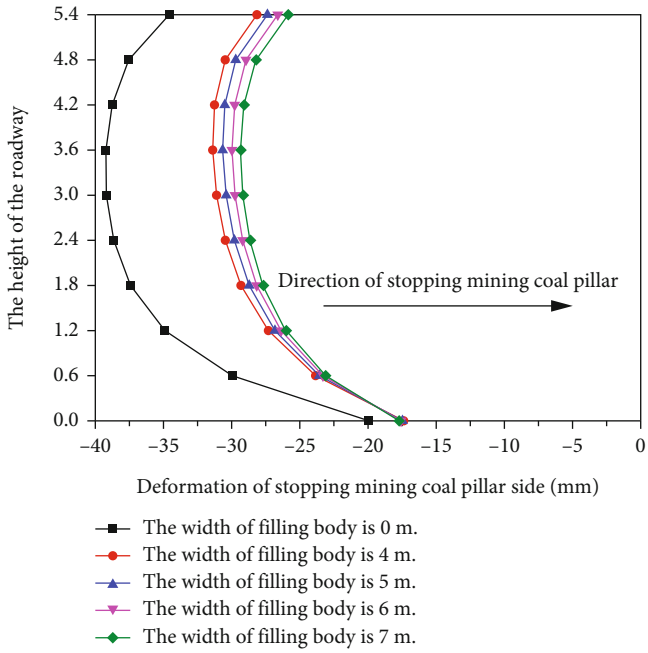

Figure 13: The deformation of the coal wall at the side of the stopping mining coal pillar in the auxiliary main haulage roadway.

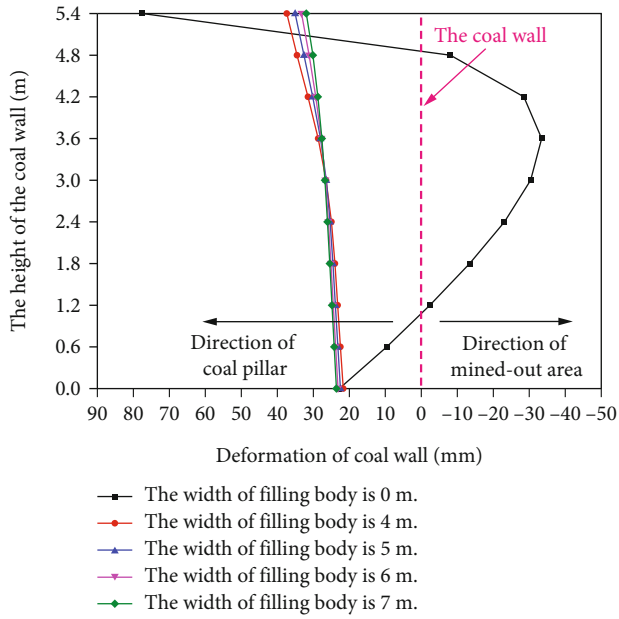

Figure 14: The coal wall deformation at the side of the stopping mining coal pillar in the retracement channel.

5. Engineering Practice

5.1. Roadway Supporting Structure. The 6105 working face of Hongshuliang Coal Mine adopts the scheme that the width of the "filling body-remaining coal pillar" structure

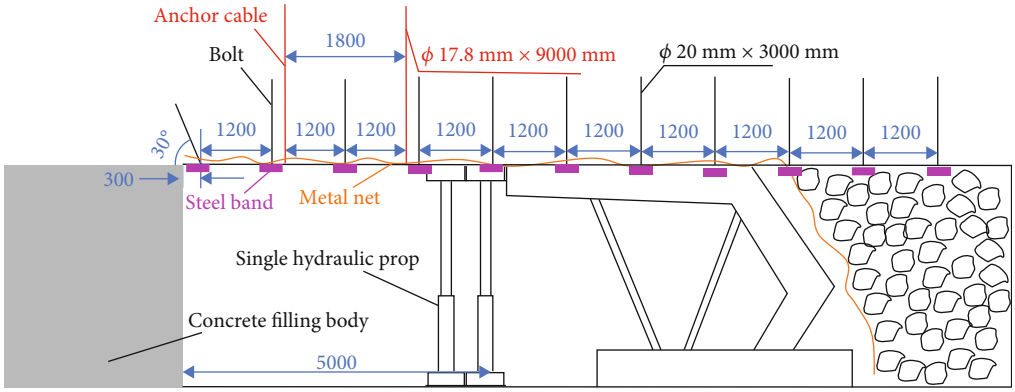

Figure 15: Supporting schematic diagram of retracement channel.

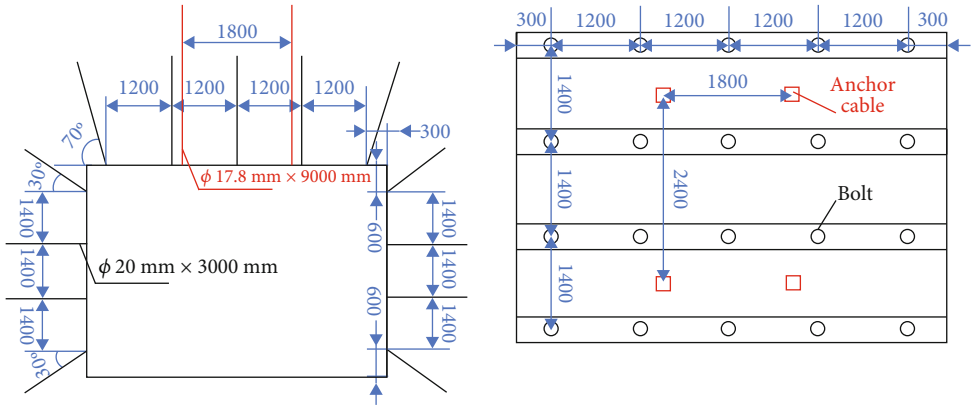

(a) Section diagram of roadway

(b) The plan of the roadway

Figure 16: Schematic diagram of support in the auxiliary main haulage roadway.

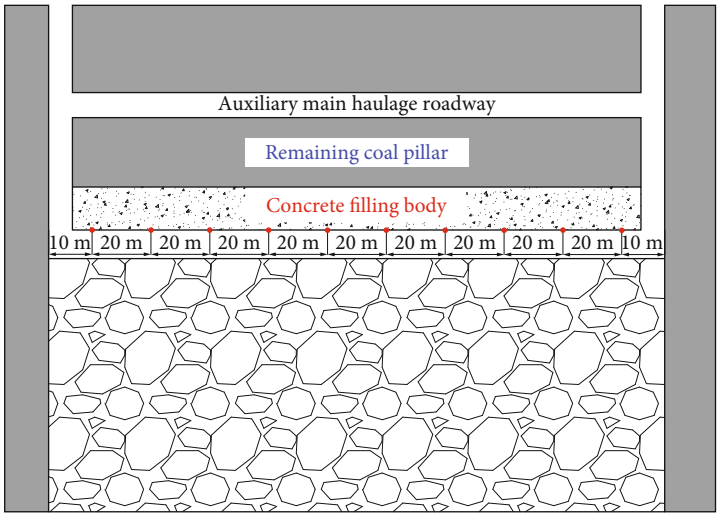

Figure 17: The schematic diagram of measuring point position.

is 25 m, and the width of concrete filling body with uniaxial compressive strength being 50 MPa is 6 m. The supporting structure used in the retracement channel is the combined supporting form of bolt, anchor cable, metal mesh, steel strip, and single hydraulic prop. The specifications, spacing, and row spacing of the bolt are ϕ20mm × 3000 mm, 1200 mm, and 1200 mm, respectively. The specifications, spacing, and row spacing of the anchor cable are ϕ17.8 mm × 9000 mm, 1800 mm, and 2400 mm, respectively. The supporting structure of the retracement channel is shown

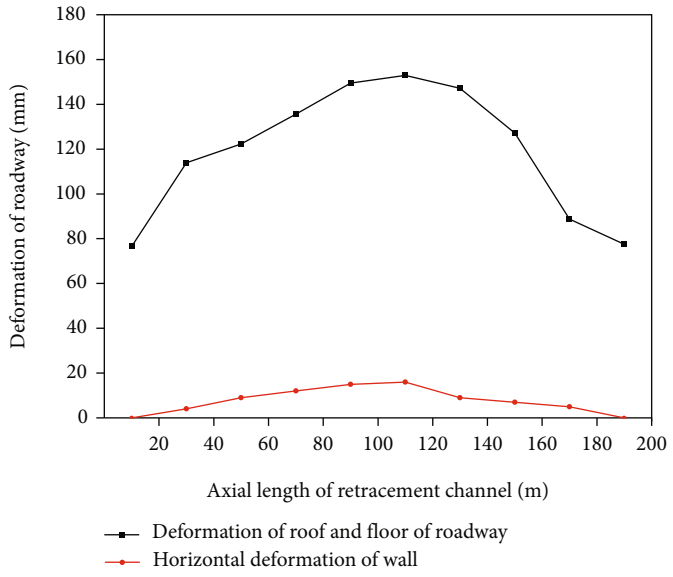

Figure 18: Deformation of retracement channel.

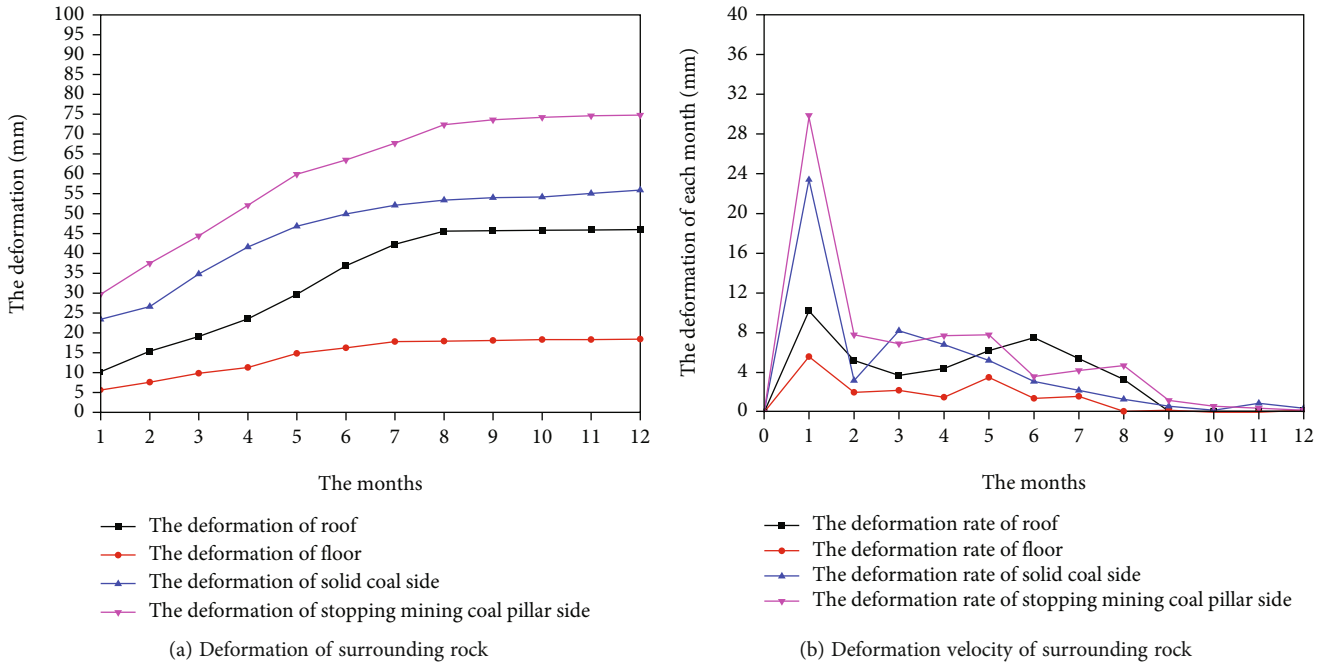

(a) Deformation of surrounding rock

(b) Deformation velocity of surrounding rock

Figure 19: The surrounding rock deformation and deformation speed of the auxiliary main haulage roadway.

in Figure 15. The combined support of bolt, anchor cable, metal mesh, and steel belt is adopted in the auxiliary main haulage roadway. The specifications, spacing, and row spacing of the roof bolt are ϕ20mm × 3000 mm, 1800 mm, and 2400 mm, respectively. The specifications, spacing, and row spacing of the roof anchor cable are φ17.8 mm × 9000 mm, 1800 mm, and 2400 mm, respectively. In the two sides of the auxiliary main haulage roadway, the specifications, spacing, and row spacing of the bolt are φ20mm × 3000 mm, 1400 mm, and 1400 mm, respectively. The supporting structure of the auxiliary main haulage roadway is shown in Figure 16.

5.2. Deformation of Surrounding Rock. When the working face is connected with the retracement channel, the deformation of the surrounding rock of the retracement channel is measured according to the location of the measuring point in Figure 17, and the deformation of the surrounding rock of the retracement channel is shown in Figure 18.

As shown in Figure 18, in the axial direction of the retracement channel, the surrounding deformation of the retracement channel is the distribution trend of small deformation at both ends and large deformation in the middle. In the axial direction of the retracement channel, the deformation between the roof and floor at both ends

of the retracement channel is 76.6 mm and 77.5 mm, respectively, and the deformation between the roof and floor in the middle is 152.9 mm. In the axial direction of the retracement channel, the horizontal deformation of the filling body at both ends of the retracement channel is 0 mm, and the horizontal deformation of the filling body in the middle is 16 mm.

The mining work of the 6105 working face is finished, and the deformation of the auxiliary main haulage roadway for one year is monitored. The surrounding rock deformation and deformation speed of the auxiliary main haulage roadway are shown in Figure 19.

It can be seen from Figure 19 that the deformation rate of surrounding rock of the auxiliary main haulage roadway increases first and then decreases. After eight months, the deformation of surrounding rock of the auxiliary main haulage roadway tends to be stable. In the auxiliary main haulage roadway, the maximum deformations of roof, floor, solid coal side, and stopping mining coal pillar side are 46 mm, 18.4 mm, 55.9 mm, and 74.8 mm, respectively, which meets the safety in production requirements of the mine. Compared with the stopping mining coal pillar in the previous working face, the recovery rate of stopping mining coal pillar increased by 52.5%.

6. Conclusions

(1) Based on the "┤" type spatial structure of stop mining position of working face, the mechanical equilibrium model is established. By using the synergistic effect of "filling body-remaining coal pillar" structure, the width formula of the of "filling body-residual coal pillar" structure is deduced

(2) The "filling body-remaining coal pillar" structure sharing the load of the overlying rock mass can improve the stability of the stopping mining coal pillar, enhance the stability of the surrounding rock of the auxiliary main haulage roadway and retracement channel, and eliminate the spalling and large deformation of the surrounding rock of the retracement channel

(3) Comprehensive analysis shows that the width of "filling body-residual coal pillar" structure is 25 m, in which the width of concrete with uniaxial compressive strength of 50 MPa is 6 m that can ensure the long-term stability of coal pillar. Compared with the stopping mining coal pillar in the previous working face, the recovery rate of stopping mining coal pillar increased by 52.5%

(4) Field measurement shows that when the working face and the retracement channel are connected, the deformation between the roof and floor of the retracement channel is between 76.6 mm and 152.9 mm, and the horizontal deformation of the filling body is between 0 mm and 16 mm. In the auxiliary main haulage roadway, the maximum deformations of roof, floor, solid coal side, and stopping mining coal pillar side are 46 mm, 18.4 mm, 55.9 mm, and 74.8 mm, respectively, which meets the safety in production requirements of the mine

Data Availability

The data used to support the findings of this study are available from the corresponding author upon request.

Conflicts of Interest

The authors declare no conflicts of interest.

Acknowledgments

This paper is supported by the National Natural Science Foundation of Surface Project of China (No. 51774289), the National Natural Science Foundation of the Youth Science Foundation of China (No. 51404270), the Open Fund of State Key Laboratory of Green and Safe Development of Western Coal (SKLCRKF1903), and the National Natural Science Foundation of Surface Project of China (No. 52074291).

References

[1] X. Sun and T. Wang, "Study the large mining height of end-mining coal pillar of fully mechanized caving in extra-thick coal seam," *Shandong Coal Science and Technology*, vol. 11, no. 3, pp. 21–23, 2015.

[2] X. Wang, J. Li, X. Zhao, and Y. Liang, "Propagation characteristics and prediction of blast-induced vibration on closely spaced rock tunnels," *Tunnelling and Underground Space Technology*, vol. 123, article 104416, 2022.

[3] C. An-ye, D. Lin-ming, L. Fu-chen, J. Heng, Q. Yun, and H. Rong-jun, "Study on characteristic of overburden movement in unsymmetrical isolated longwall mining using microseismic technique," *Procedia Engineering*, vol. 26, pp. 1253–1262, 2011.

[4] W. A. Jin-qiang, H. U. Nai-lian, J. I. Fu-xing, L. Ü. Wen-sheng, and Q. U. Xiao-cheng, "Calculation method for the seismic wave energy of microseismic hypocenters," *Journal of University of Science and Technology Beijing*, vol. 35, no. 6, pp. 703–708, 2013.

[5] J. Sun, H. Hou, and L. Wang, "Determination of stop mining line rational position at fully mechanized mining face," *Safety in Coal Mines*, vol. 44, no. 3, pp. 44–47, 2013.

[6] J.-h. Han, C. Li, and R. Yang, "Study on the reasonable size of coal pillar of the stop mining line of in deep mine," *Shandong Coal Science and Technology*, vol. 5, pp. 9–11, 2015.

[7] K. Chen, J. B. Bo, Z. C. Hu, and Q. Zu, "Analysis of influence of advance abutment pressure on dip and rational end-mining line selection," *Coal Mining Technology*, vol. 15, no. 1, pp. 35–37, 2010.

[8] W. Y. Zhang, R. J. Jin, L. Gao, and F. H. Wang, "Location determination on mining terminal line of underlying coal pillar mining face in Seam Island and study on support of dynamic pressure gateway," *Mine Construction Technology*, vol. 41, no. 4, pp. 42–46, 2020.

[9] Y. S Li, "The rock burst control of the fully-mechanized sublevel caving mining with isolated island coal pillars,"

Hydraulic Coal Mining & Pipeline Transportation, pp. 64–66, 2011.

[10] J. H. Liu, X. J. Zheng, H. Liu, Y. Wang, X. T. Lu, and W. B. Wang, "Study on rational width of protective coal pillar for district dip in rock burst mine," *Coal Science and Technology*, vol. 49, no. 2, pp. 52–60, 2021.

[11] Z. L. Li, L. M. Dou, W. Cai et al., "Fault-pillar induced rock burst mechanism of thick coal seam in deep mining," *Chinese Journal of Rock Mechanics and Engineering*, vol. 32, no. 3, pp. 333–342, 2013.

[12] W. A. Yi, C. A. An-Ye, D. O. Lin-Ming et al., "Study on the rock burst risk caused by the irrational layout of the mining exploitation," *Journal of Mining & Safety Engineering*, vol. 29, no. 6, pp. 827–832, 2012.

[13] W. Shi, J. Zhang, H. Zhang, and Y. Liu, "Structural division and determination of rational width for water proof partition coal pillar," *Journal of Rock Mechanics and Engineering*, vol. 36, no. 5, pp. 1227–1237, 2017.

[14] W. A. Fang-Tian, T. U. Shi-Hao, T. U. Hong-Sheng, L. I. Zhao-Xin, and C. H. Fang, "Mutation instability mechanism of the room mining residual pillars in the shallow depth seam," *Journal of Mining and Safety Engineering*, vol. 29, no. 6, pp. 770–775, 2012.

[15] S. J. Chen, D. W. Yin, B. L. Zhang, H. F. Ma, and X. Q. Liu, "Mechanical characteristics and progressive failure mechanism of roof-coal pillar structure," *Journal of Rock Mechanics and Engineering*, vol. 36, no. 7, pp. 1588–1598, 2017.

[16] H. Yanli, Z. Jixiong, A. Baifu, and Z. Qiang, "Overlying strata movement law in fully mechanized coal mining and backfilling longwall face by similar physical simulation," *Journal of Mining Science*, vol. 47, no. 5, pp. 618–627, 2011.

[17] Q. Minggao, S. Pingwu, and X. Jialin, "Ground pressure and strata control," China University of Mining and Technology Press, Xuzhou, 2010.

[18] J. He, L. M. Dou, A. Y. Cao, S. Y. Gong, and J. W. Lü, "Rock burst induced by roof breakage and its prevention," *Journal of Central South University of Technology*, vol. 19, no. 4, pp. 1086–1091, 2012.

[19] J. F. Shao, Q. Z. Zhu, and K. Su, "Modeling of creep in rock materials in terms of material degradation," *Computers and Geotechnics*, vol. 30, no. 7, pp. 549–555, 2003.

[20] D. F. Malan, "Manuel rocha medal recipient simulating the time-dependent behaviour of excavations in hard rock," *Rock Mechanics*, vol. 35, no. 4, pp. 225–254, 2002.

[21] P. Feng, F. Dai, Y. Liu, N. Xu, and P. Fan, "Effects of coupled static and dynamic strain rates on mechanical behaviors of rock-like specimens containing pre-existing fissures under uniaxial compression," *Canadian Geotechnical Journal*, vol. 55, no. 5, pp. 640–652, 2018.

[22] Y. Xu, F. Dai, and H. Du, "Experimental and numerical studies on compression-shear behaviors of brittle rocks subjected to combined static-dynamic loading," *International Journal of Mechanical Sciences*, vol. 175, article 105520, 2020.

[23] J. Zhang, X. Miao, X. Mao, and Z. Chen, "Research on waste substitution extraction of strip extraction coal-pillar mining," *Chinese Journal of Rock Mechanics and Engineering*, vol. 26, Supplement 1, pp. 2687–2693, 2007.

[24] S. J. Chen, W. J. Guo, and G. H. Wen, "Structure model and movement law of overburden during strip pillar mining backfill with cream-body," *Journal of China Coal Society*, vol. 36, no. 7, pp. 1081–1086, 2011.

[25] J. X. Zhang, X. J. Deng, X. Zhao, F. Ju, and B. Y. Li, "Effective control and performance measurement of solid waste backfill in coal mining," *International Journal of Surface Mining Reclamation and Environment*, vol. 31, no. 2, pp. 91–104, 2016.

[26] S. J. Chen, W. J. Guo, H. Zhou, B. Shen, and J. B. Liu, "Field investigation of long-term bearing capacity of strip coal pillars," *International Journal of Rock Mechanics and Mining Sciences*, vol. 70, pp. 109–114, 2014.

[27] Z. Jincai, G. Xinhe, and X. Kuiren, "Study on stability of coal pillar in strip mining," *Journal Of Mining And Strata Control Engineering*, vol. 4, pp. 21–25, 1994.

[28] X. Yin, S. Yan, and Y. An, "Characters of the rib spalling in fully mechanized caving face with great mining height," *Journal of Mining and Safety Engineering*, vol. 25, no. 2, pp. 222–225, 2008.

[29] D. Chen and X. Hua, "Large height mining working face Coal Wall rib spalling lever stability analysis," *Coal and Chemical Industry*, vol. 37, no. 1, pp. 30–32, 2014.

[30] Y. L. Tan, F. H. Yu, J. G. Ning, and T. B. Zhao, "Design and construction of entry retaining wall along a gob side under hard roof stratum," *International Journal of Rock Mechanics and Mining Sciences*, vol. 77, pp. 115–121, 2015.

[31] G. U. Shuancheng, H. U. Rongbin, L. I. Jinhua, and S. U. Peili, "Stability analysis of un-mined coal pillars during the pressure adjustment prior to working face transfixion," *Journal of Mining and Safety Engineering*, vol. 34, no. 1, pp. 60–66, 2017.

[32] H. Y. Zhang, "Study on Reasonable Size of Protective Coal Pillars in Mining Area Dip," *Coal Engineering*, vol. 34, no. 11, pp. 82–88, 2014.

[33] Y. Tan, W. B. Guo, and Y. H. Zhao, "Engineering stability and instability mechanism of strip Wongawilli coal pillar system based on catastrophic theory," *Journal of China Coal Society*, vol. 41, no. 7, pp. 1667–1674, 2016.